Determination of Effective Flash Stimulation Frequency and EEG Channels with Machine Learning Algorithms to Detect Migraine in Children

Çocuklarda Migren Tespiti İçin Işıklı Uyarım Frekansı ve EEG Kanallarının Belirlenmesi: Makine Öğrenmesi Algoritmaları ile Bir Yaklaşım

Aysel Burcu İBİLİ[1*] (iD), **Uğur FİDAN[2]** (iD), **Emin İBİLİ[3]** (iD), **Dilek ÇAVUŞOĞLU[4]** (iD), **Neşe Ö. YILMAZ[5]** (iD), **Nurullah OKUMUŞ[6]** (iD)

[1] Uşak Üniversitesi, Çocuk Sağlığı ve Hastalıkları Anabilim Dalı, Uşak, Türkiye
[2] Afyon Kocatepe Üniversitesi, Mühendislik Fakültesi, Biyomedikal Mühendisliği Bölümü, Afyonkarahisar, Türkiye
[3] Afyonkarahisar Sağlık Bilimleri Üniversitesi, Sağlık Yönetimi Bölümü, Afyonkarahisar, Türkiye
[4] Afyonkarahisar Sağlık Bilimleri Üniversitesi Hastanesi, Pediatrik Nöroloji Anabilim Dalı, Afyonkarahisar, Türkiye
[5] Afyon Kocatepe Üniversitesi, Mühendislik Fakültesi, Biyomedikal Mühendisliği Bölümü, Afyonkarahisar, Türkiye
[6] Afyonkarahisar Sağlık Bilimleri Üniversitesi, Afyonkarahisar, Türkiye

Abstract

This study aims to evaluate the usability of electroencephalography (EEG) data obtained under photic stimulation in diagnosing pediatric migraine. EEG data from 20 children diagnosed with migraine and 18 healthy controls aged 6–18 years were analyzed. EEG recordings were acquired using the OpenBCI Cyton+Daisy system, and photic stimulation at increasing frequencies between 2–16 Hz was applied. Data were analyzed using the wavelet transform method, and significant arousal patterns were detected in FP1, FP2, T5, and T6 channels. Classification with Support Vector Machine (SVM) and Multilayer Artificial Neural Network (ANN) algorithms revealed that the SVM method achieved the highest accuracy (76.35%) at 6 Hz, while the ANN method achieved 79.05% accuracy at 12 Hz. The findings suggest that EEG data can reveal distinct patterns at different frequencies and channels in pediatric migraine patients. The results align partially with adult migraine studies, yet the prominent response at 6 Hz and 12 Hz in children highlights the study's unique contribution. This research underscores the potential of EEG-based artificial intelligence methods for early diagnosis and monitoring of pediatric migraine, offering a novel perspective to the literature.

Keywords: Migraine, Children EEG, Wavelet Transformi, Machine Learning, Support Vector Machine

Öz

Bu çalışma, çocukluk çağı migren hastalarında elektroensefalografi (EEG) verilerinin ışıklı stimülasyon altında analiz edilerek migren tanısında kullanılabilirliğini değerlendirmeyi amaçlamaktadır. Çalışmada, 6–18 yaş aralığında migren tanısı almış 20 çocuk ve 18 sağlıklı kontrol olgusunun EEG verileri incelenmiştir. EEG kayıtları OpenBCI Cyton+Daisy cihazı kullanılarak elde edilmiş ve 2–16 Hz arasında artan frekanslarda ışıklı stimülasyon uygulanmıştır. Veriler dalgacık dönüşümü yöntemiyle analiz edilmiş, FP1, FP2, T5 ve T6 kanallarında anlamlı uyarılma paternleri tespit edilmiştir. Destek Vektör Makineleri (SVM) ve Çok Katmanlı Yapay Sinir Ağı (ANN) algoritmaları kullanılarak yapılan sınıflandırmalarda, SVM yöntemi 6 Hz frekansında %76,35 doğruluk oranı ile en iyi sonucu verirken, ANN yöntemi 12 Hz frekansında %79,05 doğruluk sağlamıştır. Bulgular, çocukluk çağı migren hastalarında EEG verilerinin farklı frekans ve kanallarda anlamlı paternler oluşturabileceğini göstermiştir. Ayrıca, elde edilen sonuçlar, yetişkin migren çalışmalarındaki bulgularla kısmen uyum göstermekte, ancak çocuk hastalarda 6 Hz ve 12 Hz frekanslarının öne çıkması çalışmanın özgün katkısı olarak değerlendirilmektedir. Bu çalışma, çocukluk çağı migreninin erken tanı ve izlenmesinde EEG tabanlı yapay zeka yöntemlerinin potansiyelini vurgulamakta ve literatüre yeni bir perspektif sunmaktadır.

Anahtar Kelimeler: Migren, Çocuk EEG, Dalgacık Dönüşümü, Makine Öğrenmesi, Destek Vektör Makinesi

1. Introduction

Migraine is a common primary headache disorder in childhood and adolescence, with a reported prevalence ranging from 30% to 57% among pediatric populations (Kilic, 2021). Diagnosing migraine in children poses a clinical challenge due to the nonspecific nature of symptoms and the difficulty in obtaining reliable patient history. This diagnostic complexity can lead to misdiagnoses and confusion with other neurological disorders such as epilepsy (Rho et al., 2020). The phenotypic overlaps between migraine and epilepsy have heightened the diagnostic relevance of

electroencephalography (EEG) in differentiating these conditions (Kamaşak et al., 2018). EEG, as a non-invasive neurophysiological technique, provides valuable insights into migraine pathophysiology, particularly when applied during photic stimulation protocols (Raghuraman and Joshi, 2024). In migraine patients, especially children, frequent EEG findings include abnormalities in the frontal and temporal regions, increased cortical excitability, and decreased alpha wave activity (Klein et al., 2024; Abdurrahman and Keane, 2024). Recent advances have demonstrated that the application of machine learning (ML) and deep learning (DL) techniques to EEG data offers a promising direction for migraine diagnosis (Petrušić et al., 2024; Ashokan et al., 2025). Artificial neural networks have shown high accuracy in distinguishing migraine subtypes (Reddy and Reddy, 2025), while random forest algorithms have proven effective even in low-resource healthcare settings (Ashokan et al., 2025). These developments emphasize the growing importance of integrating AI-assisted methods into clinical diagnostic workflows.

Despite these advancements, the majority of EEG and ML-based migraine studies have predominantly focused on adult populations, leaving a significant gap in pediatric-focused research (Kazemi and Katibeh, 2018; Rho et al., 2020; Guarnera et al., 2021). This gap highlights the urgent need for novel diagnostic approaches tailored to children. For instance, Kazemi and Katibeh (2018) compared parametric and non-parametric EEG feature extraction methods in pediatric migraine patients but did not incorporate photic stimulation protocols or advanced analytical techniques. Rho et al. (2020) reported EEG anomalies in pediatric headache cases but did not evaluate stimulus-related EEG responses or ML-based classifications. Meanwhile, Guarnera et al. (2021) investigated cortical thickness and gyrification alterations using MRI, but did not utilize EEG or implement AI-driven classification models.

This study aims to determine the optimal flash stimulation frequency and duration for EEG-based classification of pediatric migraine. By leveraging support vector machines (SVMs) and artificial neural networks (ANNs), the study seeks to enhance diagnostic accuracy. The findings are expected to contribute to the growing body of research supporting the use of EEG and machine learning algorithms in the early and non-invasive diagnosis of migraine in children.

2. Materials and Methods

This study aimed to acquire EEG recordings under photic stimulation protocols in pediatric patients diagnosed with migraine and to analyze the resulting data using machine learning techniques. The experimental methods employed in the study are described in detail to ensure reproducibility.

2.1 Sample

This study included 20 pediatric patients aged between 6 and 18 years who were diagnosed with migraine according to the criteria of the International Headache Society (IHS), along with 18 healthy children as the control group. The mean age of the participants was 12 ± 3.6 years, and the total sample consisted of 23 girls and 15 boys. Three children from the control group were excluded due to complaints of headache and medication use, while two children from the migraine group were excluded due to inadequate electrode contact during EEG recordings.

2.2 EEG recording method and stimulation protocol

EEG recordings were performed using the longitudinal bipolar ("double banana") montage in accordance with the international 10–20 electrode placement system. The device used was the Cyton+Daisy biosensor module by OpenBCI, offering 16 channels and a sampling rate of 250 Hz. The following electrode sites were utilized during recording: FP1, FP2, C3, C4, T3, T4, T5, T6, O1, O2, F3, F4, F7, F8, P3, and P4. Participants were exposed to photic stimulation at sequential frequencies of 2, 4, 6, 8, 10, 12, 14, and 16 Hz. Each stimulation lasted for 10 seconds, followed by a 10-second rest period. EEG signals were recorded across three-time windows: pre-stimulation, during stimulation, and post-stimulation. The system topology used in this study is illustrated in Figure 1.

EEG measurements were performed in accordance with the international 10–20 electrode placement system using a longitudinal bipolar ("double banana") montage configuration. EEG signals were acquired via the Cyton+Daisy biosensor module developed by OpenBCI, an open-source, portable EEG system with a maximum sampling rate of 250 Hz. Recordings were obtained through a 16-channel configuration. During EEG acquisition, participants were exposed to photic stimulation at sequential frequencies of 2, 4, 6, 8, 10, 12, 14, and 16 Hz. The stimulation protocol was designed to start at 2 Hz and increase in 2-Hz increments up to 16 Hz. Each stimulation period lasted 10 seconds, followed by a 10-second resting interval.

Following the light stimulation protocol, migraine patients were classified into photophobic and non-photophobic subgroups. EEG data were collected in three distinct phases: (i) pre-stimulation (baseline), (ii) during
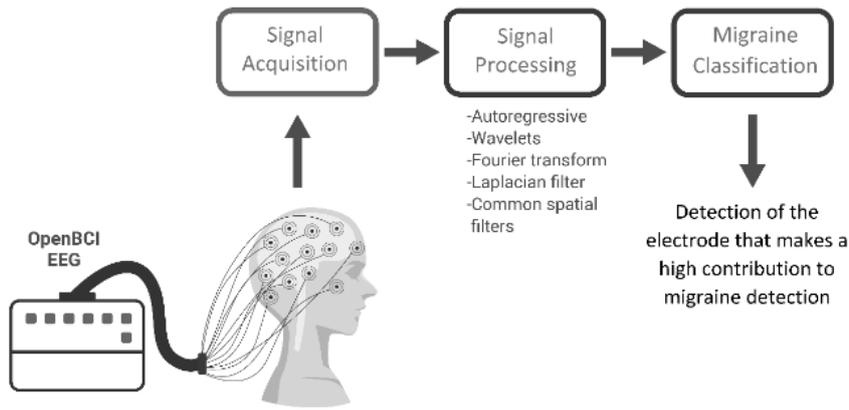
Figure 1. Operational principle of the migraine detection system (Sadeghi and Maleki, 2018).

stimulation (active), (iii) post-stimulation (post-active). Data acquisition was performed using the OpenBCI Cyton+Daisy module, and all recorded EEG signals were analyzed using MATLAB 2019.

2.3 Data collection method

2.4 Support vector machine (SVM)

SVM is supervised machine learning algorithms developed based on statistical learning theory (Vapnik, 1995). The primary objective of the SVM algorithm is to identify the optimal decision boundary that separates data points belonging to two different classes. This boundary, known as the hyperplane, is constructed on a feature space defined by the training data and serves to distinguish between the two classes with maximum margin.

SVM can be applied not only to classification problems but also to regression tasks. Due to their ability to effectively manage high-dimensional datasets, SVM is particularly well-suited for binary classification problems. A schematic illustration of the working principle of the SVM algorithm is presented in Figure 2.

2.5 Artificial neural networks (ANNs)

ANNs are algorithms inspired by the functioning of the human brain and neural cells. ANNs are widely used for modeling nonlinear phenomena and are particularly effective in solving problems for which no explicit mathematical formula or rule exists. An ANN consists of processing units (neurons) and the connections that link them. The system operates by generating an output set corresponding to a given input set. The fundamental goal of ANN is to produce new information by learning from data, enabling them to address previously unseen problems (Figure 3)
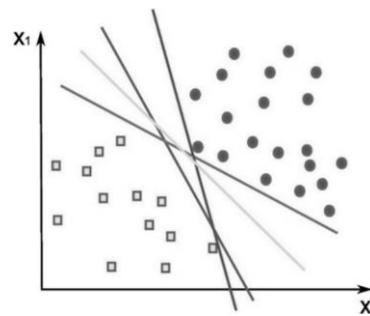

Figure 2. Basic working principle of the Support Vector Machine (SVM) algorithm (Cervantes et al., 2020).
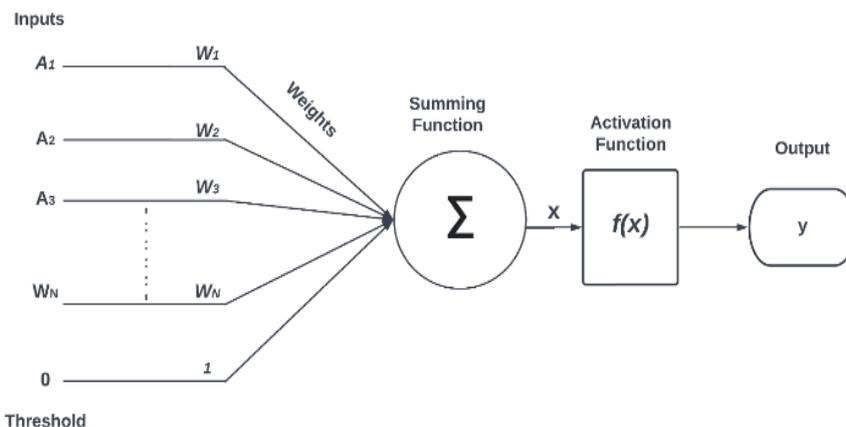

Figure 3. Artificial Neural Network (ANN) model and its fundamental components (tutorialspoint, 2024).
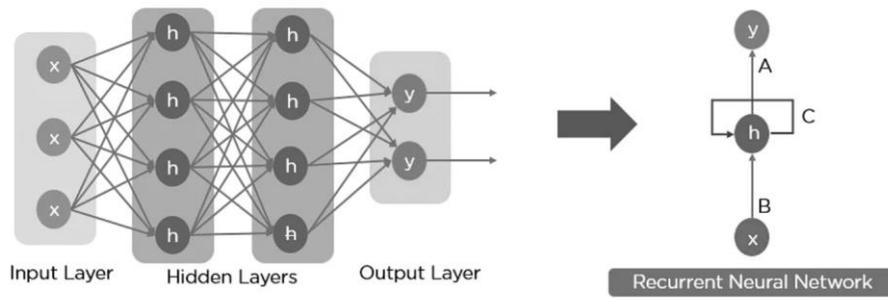
Figure 4. Multilayer perceptron (MLP) model (Ouyang et al., 2020).

- **Inputs (A):** Represent the external data fed into the artificial neuron. A = $A_0, A_1, A_2, A_3, …, A_n$

- **Weights (w):** Represent the numerical values assigned to each input, indicating the degree of influence each input has on the neuron.

w = $w_0, w_1, w_2, w_3, …, w_n$

- **Net Input (net):** The total input to the neuron, calculated as the weighted sum of all inputs. This is typically computed using the following equation.
net = $(w_0 \cdot A_0) + (w_1 \cdot A_1) + (w_2 \cdot A_2) + … + (w_n \cdot A_n)$

- **Activation Function (f(net)):** A function applied to the net input to determine the neuron's output. It decides whether the neuron should be activated based on the computed input value.
Out = f(net) = f(net) = $f((w_0 \cdot A_0) + (w_1 \cdot A_1) + (w_2 \cdot A_2) + … + (w_n \cdot A_n))$

2.6 Multilayer Artificial Neural Networks (MLP)

MLP, one of the most widely used architectures among artificial neural networks, consists of an input layer, one or more hidden layers, and an output layer. Each layer is composed of neurons (also known as nodes), and each neuron in one layer is connected to all neurons in the subsequent layer. The MLP architecture enables the modeling of complex, non-linear relationships between inputs and outputs. This structure allows the network to learn from data by adjusting the connection weights through a process known as backpropagation. During this learning process, the error between the predicted and actual outputs is propagated backward through the network to optimize weights and minimize prediction error. Each neuron in the hidden and output layers computes a weighted sum of its inputs, applies an activation function (such as sigmoid, tanh, or ReLU), and transmits the result to the next layer. The inclusion of multiple hidden layers increases the network's capacity to learn hierarchical representations of data, making MLPs particularly effective in pattern recognition, classification, and signal processing tasks.

2.7 Wavelet Transform (WT)

WT is a method used for time-frequency analysis of a signal. The Continuous Wavelet Transform (CWT) was initially developed to address challenges in the analysis of seismic data and has since been adapted for the examination of various types of signals. Similar to the Short-Time Fourier Transform (STFT), wavelet transform employs a windowing function; however, instead of a fixed window, it utilizes a "mother wavelet" function. This mother wavelet can be both scaled and translated during the transformation process. Scaling refers to compressing or stretching the wavelet, while translation denotes shifting it along the time axis. The fundamental mathematical operations of the wavelet transform may vary depending on the choice of the wavelet function and the transformation algorithm. For the Discrete Wavelet Transform (DWT), which is a sampled version of the continuous transform, the general mathematical expressions are summarized below.

- High-pass filter coefficients: h[n] = h[-n]

- Low-pass filter coefficients: $g[n] = (-1)^{(n+1)} * h[N-n-1]$, n = 0, 1, …, N-1

- Downsampling operation: x[k] = ∑(h[m] * x[2k-m]), m = 0, 1, …, N-1

- Upsampling operation: y[k] = ∑(g[m] * y[k/2-m]), m = 0, 1, …, N-1

These operations are iteratively applied to decompose and represent different frequency components of a signal. The specific equations may vary depending on the chosen wavelet function—such as Haar, Daubechies, Morlet, Symlet, Shannon, or Mexican Hat—and the transformation algorithm employed. Unlike the Short-Time Fourier Transform (STFT), the wavelet transform allows for a dynamic adjustment of the analysis window width, enhancing both time and frequency resolution. This property makes the wavelet transform a more advantageous analytical method compared to the Fourier transform, particularly for non-stationary signal analysis.

Commonly used wavelet shapes in signal processing are illustrated in Figure 5.

3. Findings

In this study, EEG data from individuals with migraine were obtained using the OpenBCI Cyton+Daisy biosensor module and a sintered electrode system. The EEG signals were recorded from the scalp in accordance with the international 10-20 electrode placement system. A representative EEG recording from a control group volunteer, acquired in the EEG laboratory, is presented in Figure 6. The configuration of the 16-channel OpenBCI Cyton+Daisy biosensor module used in the study is illustrated in Figure 7.
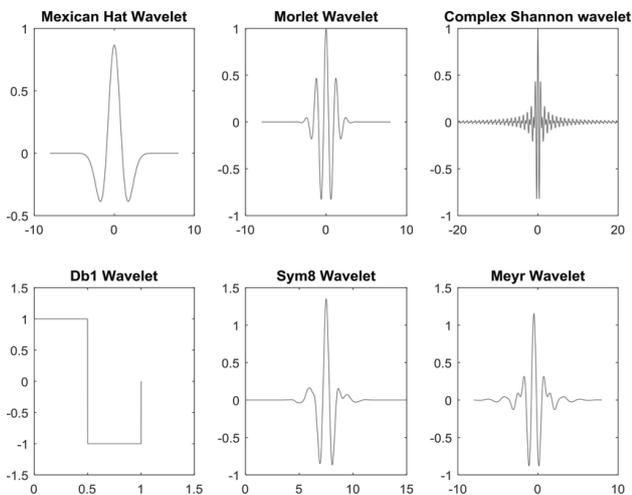
**Figure 5.** Examples of commonly used wavelet functions in wavelet transform (Dyllon and Xiao, 2018).

Figure 6. Example of EEG data acquisition from a control group volunteer.

3.1 Power spectrum density (PSD) findings

Power Spectrum Density (PSD) represents the power content of a signal as a function of frequency and is particularly useful in the characterization of broadband random signals. In this study, wavelet transform and signal processing techniques were utilized to analyze EEG signal variations across different channels for both migraine and control groups. EEG recordings were obtained from the FP1, FP2, C3, C4, T5, T6, O1, O2, F7, F8, F3, F4, T3, T4, P3, and P4 electrode sites.
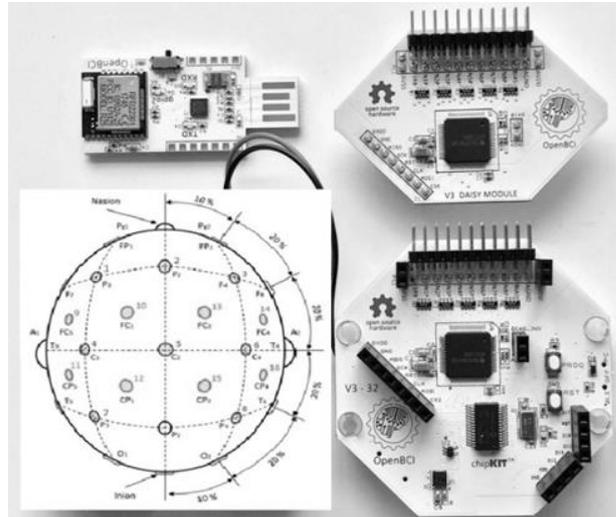

Figure 7. The 16-channel OpenBCI Cyton+Daisy biosensor module used in the study.

The wavelet-transformed data provided three-dimensional information—time, frequency, and intensity. o enable comparative evaluation, these were reduced to two-dimensional representations using power spectrum plots. In the migraine group, the EEG wave activity was observed to shift toward higher frequencies, and the intensity of wave amplitudes increased in response to photic stimulation frequencies. Notably, channels FP1, FP2, T5, and T6 demonstrated significant differences compared to other channels. Figures 8 to 10 present the power spectrum densities of both control and migraine groups before and after photic stimulation at various frequencies.

Frequency is plotted on the horizontal axis, and power values (in decibels) are presented on the vertical axis. The results reveal notable arousal-related activity in the FP1, FP2, T5, and T6 electrode channels.

3.2 Findings from the wavelet transform analysis

Figures 11–13 present the Continuous Wavelet Transform (CWT) results for both control and migraine groups at different frequencies before and after photic stimulation. It was observed that the EEG wave band frequencies in the control group were lower compared to those in the migraine group.
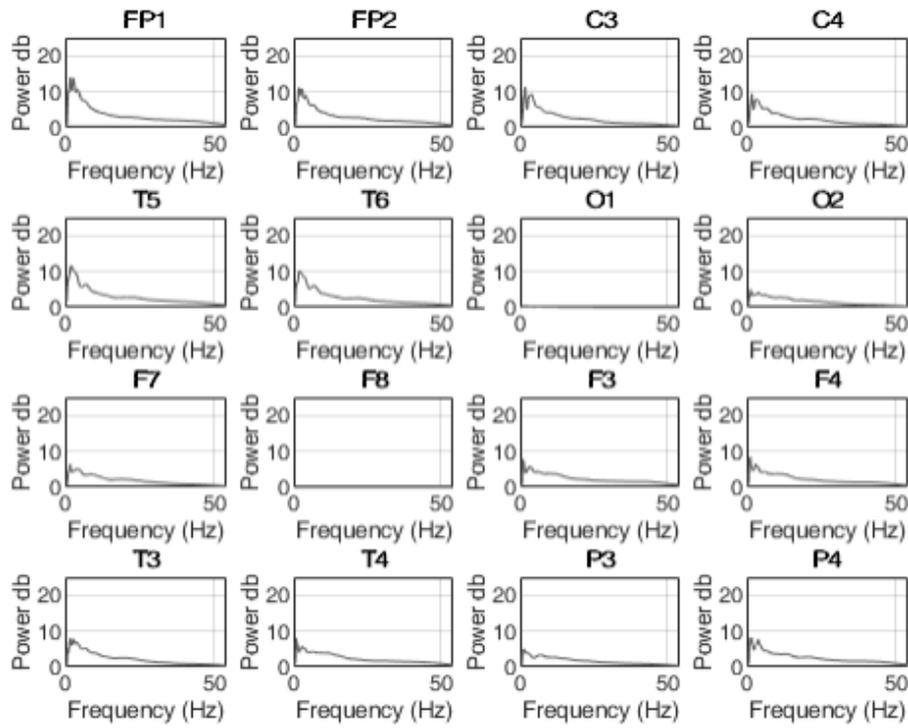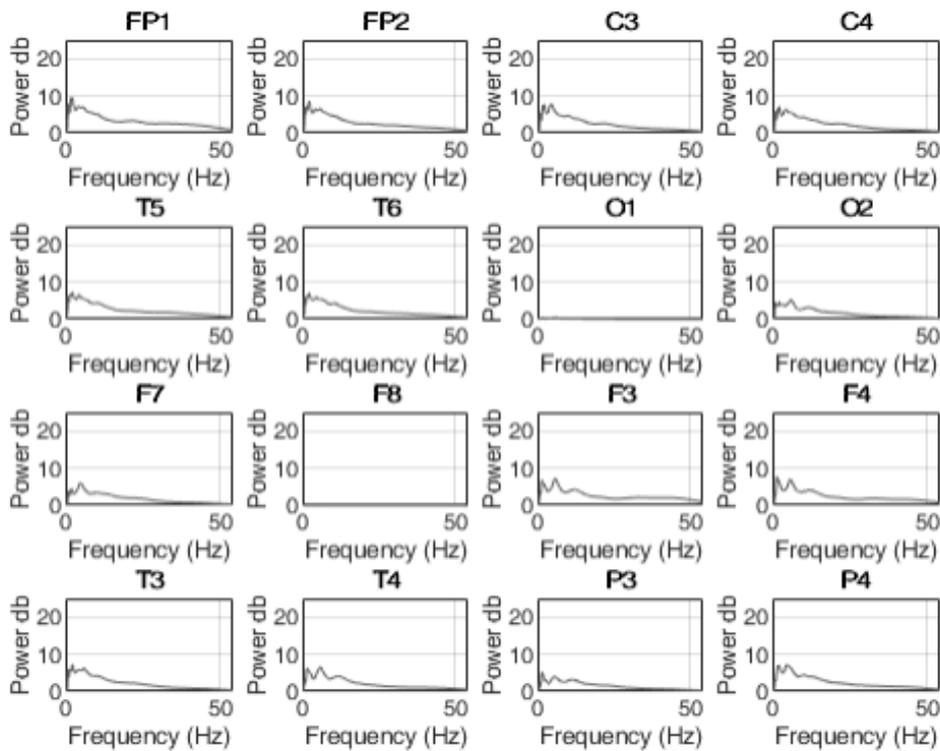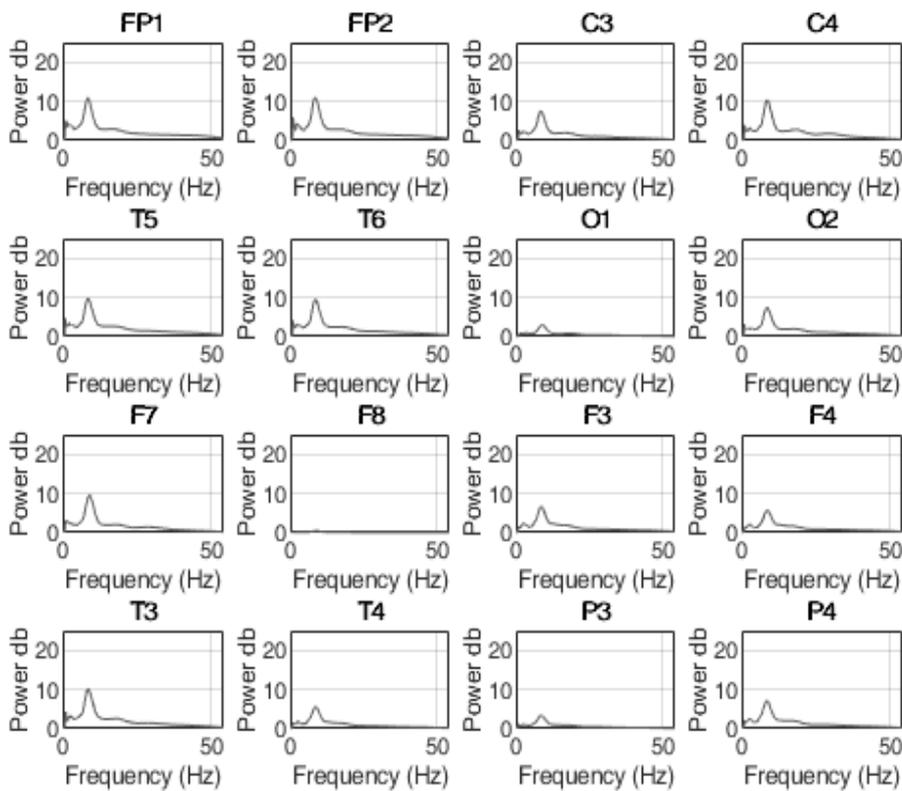
a) Control Group
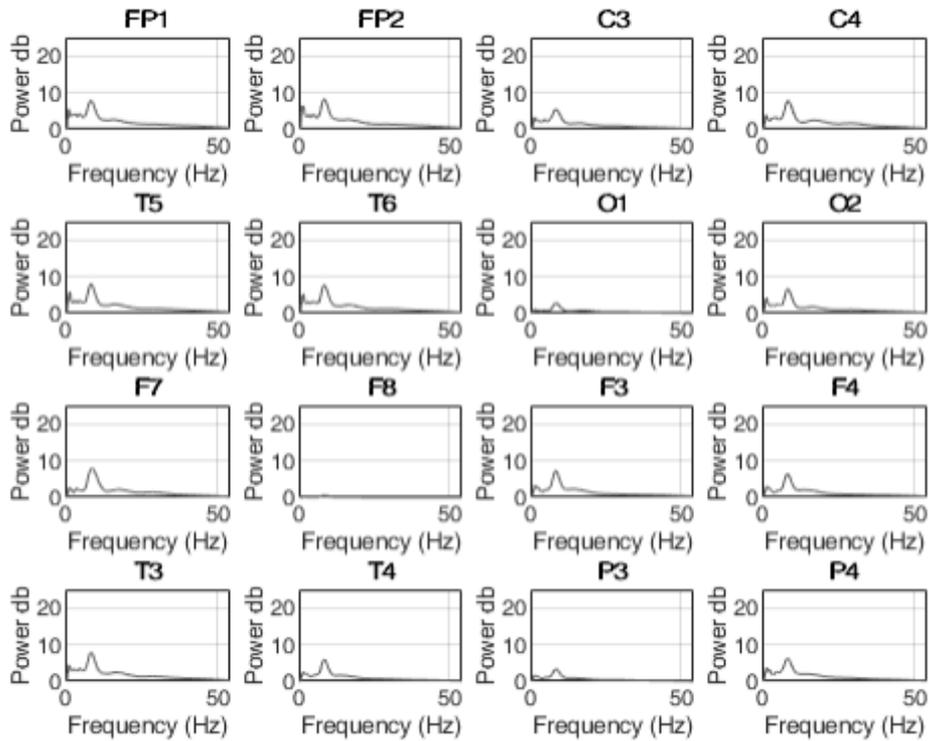
b) Migraine Group

Figure 8. Comparison of power spectrum density between the control (a) and migraine (b) groups prior to photic stimulation.
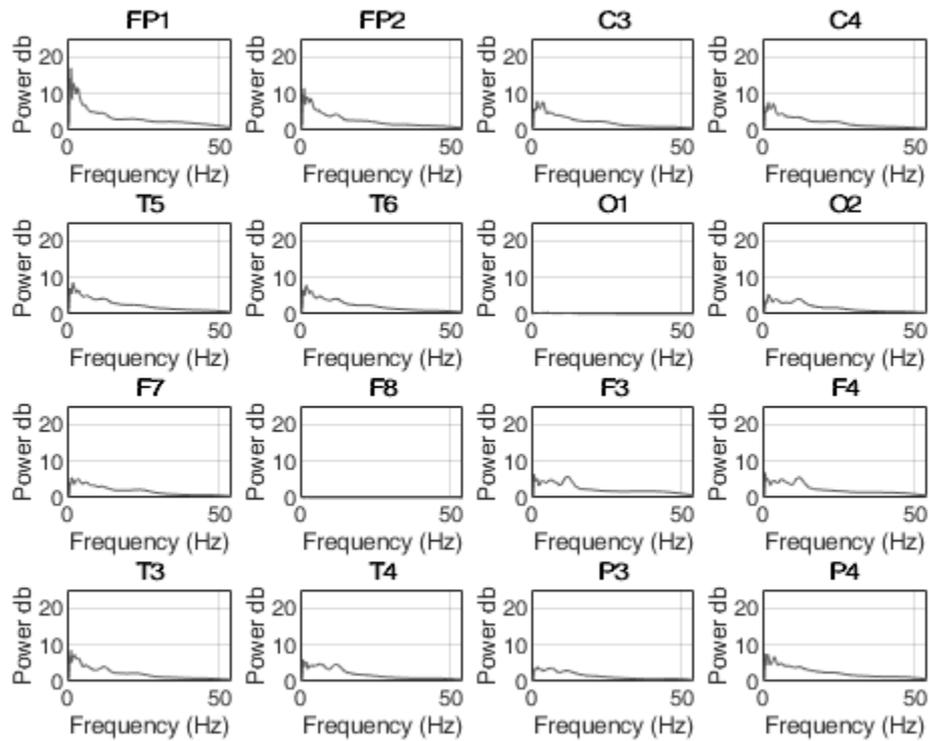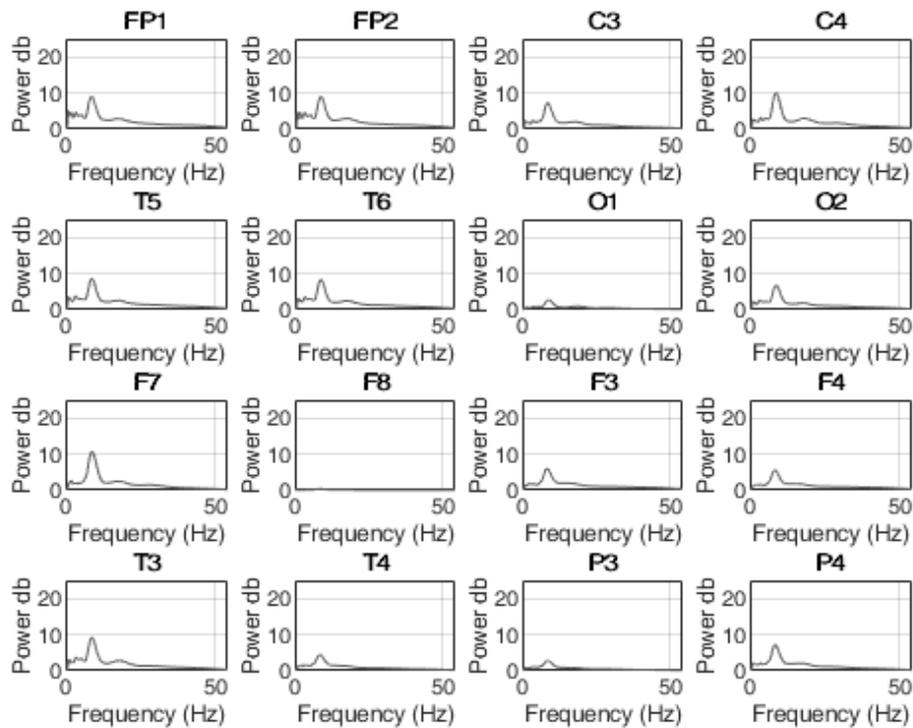
a) Control Group

b) Migraine Group

Figure 9. Comparison of power spectrum density between the control (a) and migraine (b) groups during 6Hz photic stimulation.
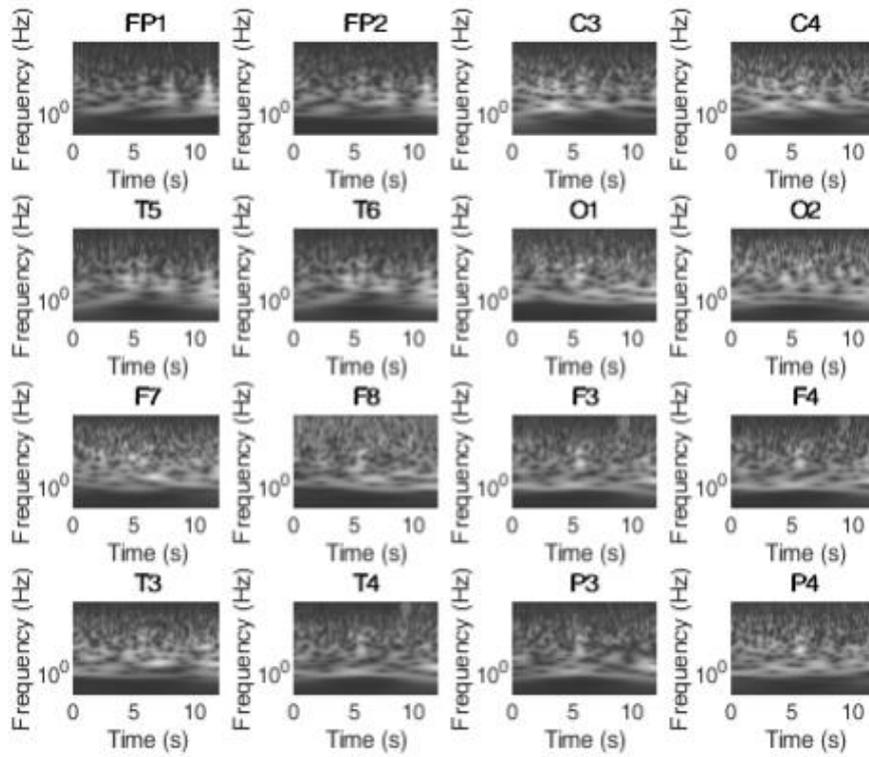
a) Control Group

b) Migraine Group

Figure 10. Comparison of power spectrum density between the control (a) and migraine (b) groups during 12 Hz photic stimulation.
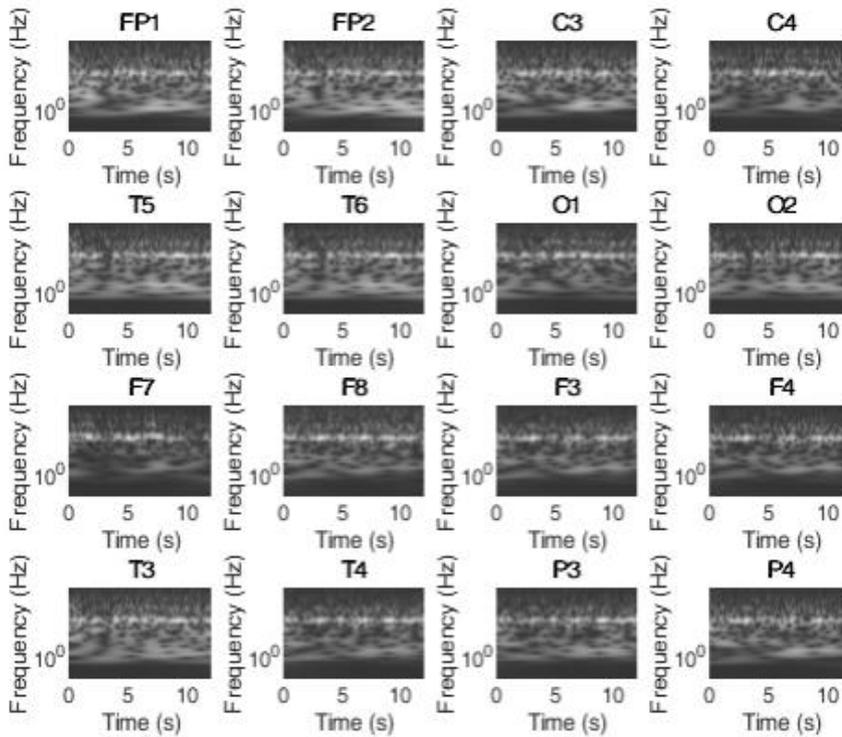
a) Control Group

b) Migraine Group

Figure 11. Wavelet transform results for the control (a) and migraine (b) groups before photic stimulation.

a) Control Group

b) Migraine Group

Figure 12. Wavelet transform results for the control (a) and migraine (b) groups during 6Hz photic stimulation.
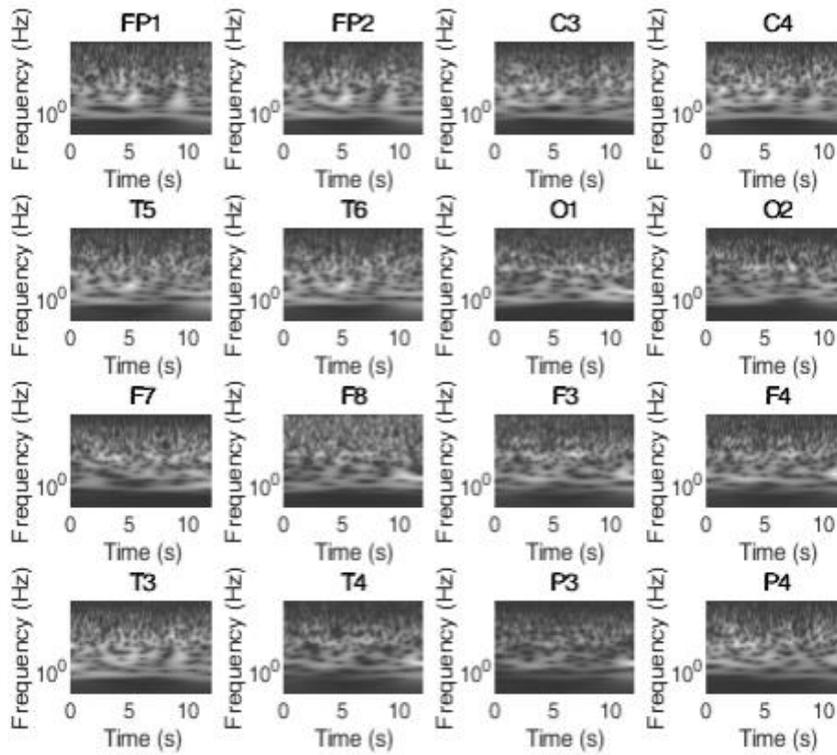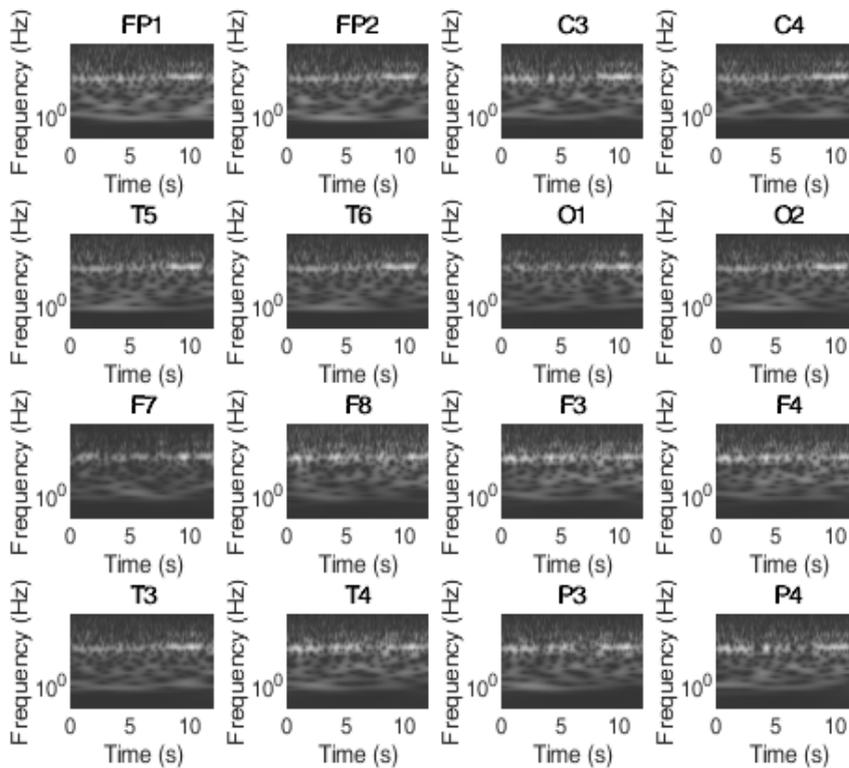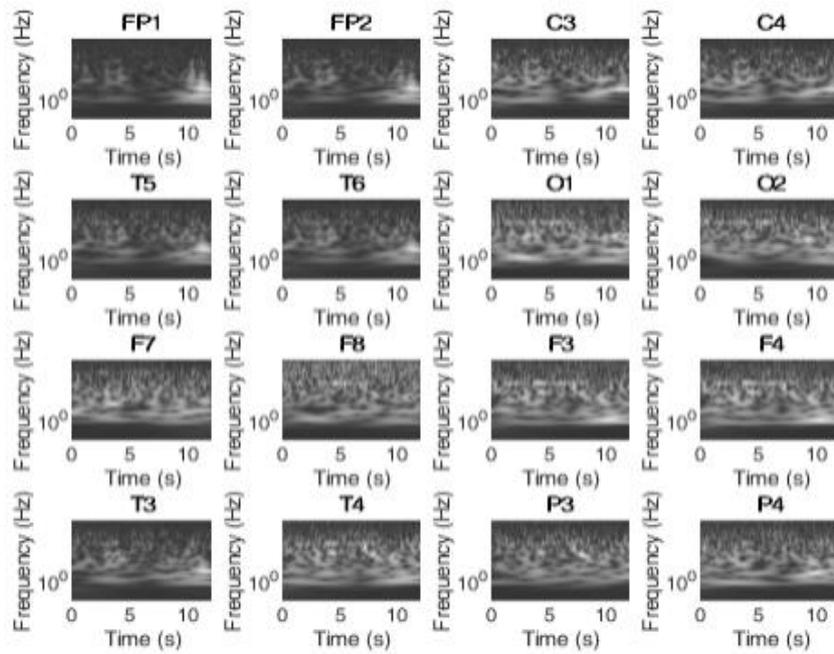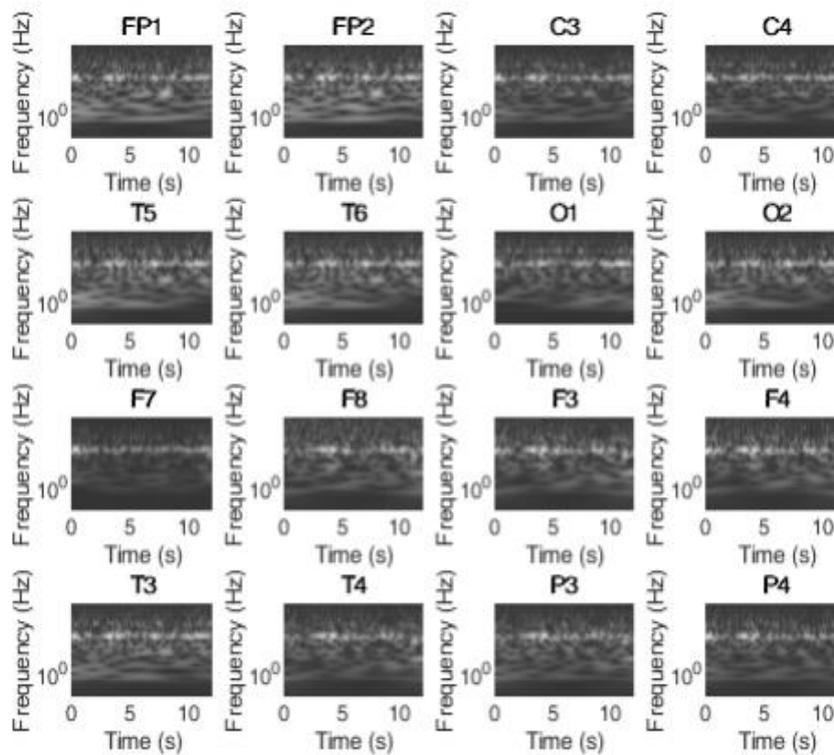
a) Control Group

b) Migraine Group

Figure 13. Wavelet transform results for the control (a) and migraine (b) groups during 12 Hz photic stimulation.

3.3 SVM and ANN algorithm results

The EEG data were analyzed using the Weka software platform, employing SVM and MLP algorithms. The data were evaluated across baseline, stimulation, and post-stimulation phases, with flash light stimuli applied at frequencies ranging from 2 Hz to 16 Hz. The analyses revealed statistically significant differences in the FP1,

FP2, T5, and T6 channels compared to other regions. **Table 1** presents the classification accuracy achieved using the SVM algorithm. Notably, at 6 Hz stimulation, a pronounced arousal response was detected in the FP1, FP2, T5, and T6 channels, yielding a classification accuracy of 76.35%. The highest average arousal responses were observed at 4 Hz and 6 Hz, suggesting these frequencies

may be particularly effective in eliciting cortical responses in pediatric migraine detection.

Table 1. Classification Accuracy of the Support Vector Machine Algorithm.

	Highest Values in Column (Bolded)				
	SVM Classifier (% Accuracy)				
	FP1	**FP2**	**T5**	**T6**	**Mean**
0	62.16	67.56	62.16	*67.56*	64.86
2 Hz	67.56	70.27	56.75	*72.97*	66.89
4 Hz	75.67	72.97	72.96	***81.08***	75.67
6 Hz	75.67	78.37	70.27	***81.08***	**76.35**
8 Hz	*72.97*	*72.97*	70.27	70.27	71.62
10 Hz	64.86	64.86	***72.97***	***72.97***	68.92
12 Hz	*78.37*	*78.37*	62.16	72.97	72.97
14 Hz	*72.97*	*72.97*	62.16	72.97	70.27
16 Hz	***81.08***	70.27	64.86	78.37	73.65
End	64.86	***86.48***	70.27	75.67	74.32
Mean	62.16	67.56	62.16	*67.56*	

Note: The highest values in each row are underlined, while the highest values in each column are bolded.

Table 2 presents the classification accuracy rates obtained using the Multilayer Perceptron (MLP) algorithm. At the 12 Hz stimulation frequency, a pronounced arousal response was observed in the FP1, FP2, T5, and T6 channels, with a classification accuracy of 79.05%. Among these, the FP1 channel exhibited the highest arousal level at 12 Hz.

Tablo 2. Classification Accuracy Rates of Multilayer Perceptron (MLP) Algorithm

	Highest Values in Column (Bolded)				
	MLP Classifier (% Accuracy)				
	FP1	**FP2**	**T5**	**T6**	**Mean**
0	*75.67*	62.16	56.75	64.86	64.86
2 Hz	*81.08*	67.56	59.45	67.56	68.91
4 Hz	75.67	78.36	70.27	*83.78*	77.02
6 Hz	75.67	64.86	67.56	***86.48***	73.64
8 Hz	*75.67*	72.97	*75.67*	70.27	73.65
10 Hz	*75.67*	59.45	64.86	54.05	63.51
12 Hz	*89.18*	75.67	**78.37**	72.97	**79.05**
14 Hz	72.97	**78.37**	72.97	*81.08*	76.35
16 Hz	*89.18*	62.16	54.05	70.27	68.92
End	72.97	*78.37*	72.97	70.27	73.65
Mean	*75.67*	62.16	56.75	64.86	

Note: The highest values in each row are underlined, and the highest values in each column are bolded.

Figure 14 presents a comparison of the results obtained from the SVM and MLP algorithms. The FP1, FP2, T5, and T6 channels exhibited prominent arousal responses across all stimulation frequencies. Notably, the highest classification accuracy was achieved at 6 Hz with the SVM algorithm (76.35%) and at 12 Hz with the MLP algorithm (79.05%).
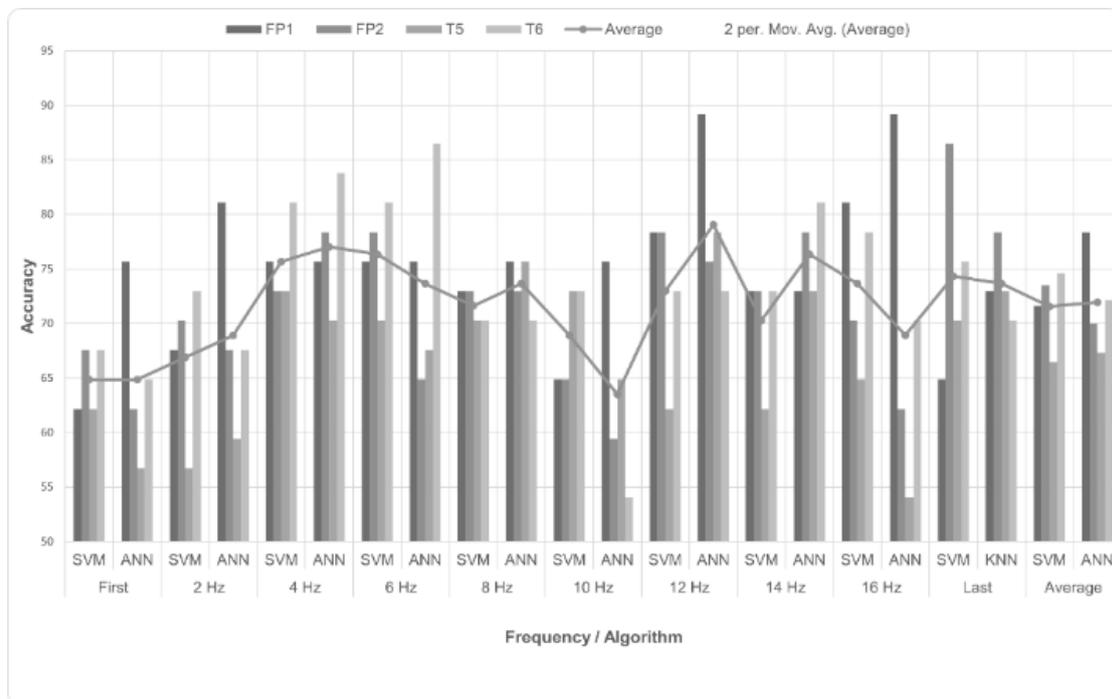
Figure 14. Comparative Accuracy Rates of SVM and MLP Algorithms in Migraine Diagnosis

3.4 General Findings

The analysis of EEG data acquired using the OpenBCI Cyton+Daisy biosensor module through signal processing and artificial intelligence techniques revealed the effects of various photic stimulation frequencies across EEG channels. The results obtained from Support Vector Machine (SVM) and Multilayer Perceptron (MLP) algorithms indicated that the FP1 and T6 channels

exhibited more pronounced arousal responses compared to the other channels. Furthermore, significant arousal activity was observed across all channels at stimulation frequencies of 4 Hz, 6 Hz, and 12 Hz.

4. Discussion and Conclusion

In this study, EEG data from pediatric migraine patients were analyzed, and significant arousal patterns were identified in response to photic stimulations at 4 Hz, 6 Hz, and 12 Hz, particularly in the FP1, FP2, T5, and T6 channels. These findings suggest that increased cortical activity in the frontal and temporal regions is more pronounced in individuals with migraine (Rocca et al., 2014; Ouyang et al., 2020; Niedermeyer & Lopes da Silva, 2020).

While the majority of EEG and machine learning-based classification studies in the literature have focused on adult migraine patients, research addressing pediatric migraine remains notably limited (Kazemi & Katibeh, 2018; Rho et al., 2020; Guarnera et al., 2021). For instance, in the study by Kazemi and Katibeh (2018), parametric and non-parametric EEG feature extraction methods were compared in children with migraine; however, no photic stimulation protocol was applied, and the analysis was restricted to conventional methods.

Similarly, the study by Rho et al. (2020) reported EEG anomalies in pediatric migraine patients but did not incorporate stimulus-related EEG changes or the use of machine learning algorithms. Guarnera et al. (2021), on the other hand, focused on cortical thickness and gyrification changes using MRI in pediatric migraine patients, without emphasizing EEG as a rapid and non-invasive method or evaluating machine learning-based classification approaches. The originality of the present study lies in its integration of EEG data recorded under photic stimulation in pediatric migraine patients, processed via Wavelet Transform, and classified using two distinct machine learning algorithms—Support Vector Machines (SVM) and Artificial Neural Networks (ANN). Moreover, the identification of arousal patterns at 4 Hz, 6 Hz, and 12 Hz stimulation frequencies extends the frequently emphasized 4 Hz finding in the literature, offering a novel contribution by highlighting additional frequency-specific responses.

When evaluated on a channel-specific basis, previous studies have frequently reported findings in channels such as O1, O2, T3, and F7 (Garcia-Chimeno et al., 2017; Kazemi & Katibeh, 2018). However, in the present study, significant arousal responses were predominantly observed in the FP1, FP2, T5, and T6 channels, suggesting

that the electrophysiological manifestations of pediatric migraine may differ in spatial distribution from those observed in adults. EEG studies on adult migraine patients have typically identified prominent activations at 4 Hz and in the beta band between T5 and T3 channels (Subasi et al., 2019). In contrast, the current study revealed marked arousal patterns not only at 4 Hz but also at 6 Hz and 12 Hz, thereby providing novel insights specific to pediatric migraine and extending the existing adult-focused literature.

Moreover, the exclusion of a participant diagnosed with epilepsy during EEG recording highlights the critical diagnostic challenge of differentiating migraine from epilepsy in pediatric populations (Kamaşak et al., 2018; Rho et al., 2020). This case supports the notion that overlapping EEG patterns between migraine and epilepsy necessitate careful interpretation in clinical practice.

The use of Wavelet Transform in this study offered higher frequency resolution compared to conventional methods such as Burg-AR and Welch, allowing for better separation of frequency components and enhanced signal detail (Gosala et al., 2023; Cordes et al., 2021). This demonstrates the significant advantage of wavelet-based analysis, particularly in complex neurological conditions such as pediatric migraine. In terms of classification performance, the SVM algorithm achieved an accuracy of 76.35% in detecting arousal at 6 Hz in the FP1, FP2, T5, and T6 channels. The ANN classifier yielded slightly higher performance with 79.05% accuracy at 12 Hz in the same channels. These findings are generally consistent with those of Garcia-Chimeno et al. (2017), who reported a 90% accuracy, and Kazemi and Katibeh (2018), who reported a 93% accuracy. However, the emphasis on FP1, FP2, T5, and T6 in the present study, as opposed to the more commonly highlighted O1, O2, T3, and F7 channels in prior literature, further reinforces the notion that pediatric migraine presents with a distinct electrophysiological signature.

In conclusion, this study demonstrates that collecting EEG data from pediatric migraine patients under photic stimulation and analyzing it using the Wavelet Transform method combined with SVM and ANN algorithms offers an effective approach for revealing the electrophysiological features of migraine. The findings suggest that EEG patterns in pediatric migraine may differ from those observed in adults, with distinct responses particularly emerging at 4 Hz, 6 Hz, and 12 Hz stimulation frequencies. Significant arousals detected in the FP1, FP2, T5, and T6 channels may serve as potential electrophysiological biomarkers for migraine diagnosis.

Future research should aim to validate these findings through studies involving larger sample sizes, broader age ranges, and longitudinal follow-up data. Additionally, standardization of photic stimulation protocols and the integration of such analytical methods into clinical guidelines are recommended to enhance diagnostic accuracy and clinical applicability.

Despite the promising classification accuracies obtained in this study (76.35% with SVM at 6 Hz and 79.05% with MLP at 12 Hz), the relatively small sample size—comprising 20 pediatric migraine patients and 18 healthy controls—represents a notable limitation. Future studies incorporating larger cohorts are recommended to improve the generalizability and robustness of the findings. Furthermore, the broad age range of the participants (6–18 years) introduces the possibility of developmental variability influencing the EEG responses. Stratifying participants into narrower age subgroups in future research may help elucidate age-dependent electrophysiological differences. While the current machine learning models demonstrated clinically acceptable performance, the application of advanced deep learning architectures such as convolutional or recurrent neural networks on larger datasets could potentially yield higher diagnostic accuracy. These enhancements would support the translation of EEG-based AI models into reliable, non-invasive tools for early pediatric migraine diagnosis.

Declaration of Ethical Standards
The authors declare that they comply with all ethical standards.

Credit Authorship Contribution Statement
Author-1: Conceptualization, Methodology, Study design, Software, Investigation, Data curation, Visualization, Writing – original draft, Supervision, Project administration.
Author-2: Formal analysis, Software, Validation, Visualization, Writing – review and editing.
Author-3: Conceptualization, Methodology, Software, Supervision, Writing – review and editing,
Author-4: Investigation, Supervision, Data curation, Resources, Visualization, Writing – review and editing.
Author-5: Resources, Validation, Data curation, Writing – review and editing.
Author-6: Supervision, Funding acquisition, Project administration, Resources.

Declaration of Competing Interest
The authors declare that they have no known competing financial interests or personal relationships that could have appeared to influence the work reported in this paper.

Data Availability Statement
All data generated or analyzed during this study are included in this published article (Datasets are available on request. The raw data supporting the conclusions of this article will be made available by the authors, without undue reservation).

5. References

Abdurrahman L, Keane M. 2024. Understanding migraine: Epidemiology, EEG abnormalities, and the potential of neurofeedback training. NeuroRegulation, 11(2):184–190. https://doi.org/10.15540/nr.11.2.184

Ashokan A, Rehman IU, Saadati P. 2025. Migraine classification using machine learning and deep learning in low-resource healthcare settings. EasyChair Preprints, 15776.

Cervantes J, Garcia-Lamont F, Rodríguez-Mazahua L, Lopez A. 2020. A comprehensive survey on support vector machine classification: Applications, challenges, and trends. Neurocomputing, 408:189-215.

Cordes D, Kaleem MF, Yang Z, Zhuang X, Curran T, Sreenivasan KR, et al. 2021. Energy-period profiles of brain networks in group fMRI resting-state data: A comparison of empirical mode decomposition with the short-time Fourier transform and the discrete wavelet transform. Front Neurosci, 15:663403.

Dyllon S, Xiao P. 2018. Wavelet transform for educational network data traffic analysis. In: Wavelet Theory and Applications, p. 155.

Garcia-Chimeno Y, Garcia-Zapirain B, Gomez-Beldarrain M, Fernandez-Ruanova B, Garcia-Monco JC. 2017. Automatic migraine classification via feature selection committee and machine learning techniques over imaging and questionnaire data. BMC Med Inform Decis Mak, 17(1):1-10.

Gosala B, Kapgate PD, Jain P, Chaurasia RN, Gupta M. 2023. Wavelet transforms for feature engineering in EEG data processing: An application on schizophrenia. Biomed Signal Process Control, 85:104811.

Guarnera A, et al. 2021. Early alterations of cortical thickness and gyrification in migraine without aura: A retrospective MRI study in pediatric patients. J Headache Pain, 22(1):79.

Kamaşak T, Durgut BD, Arslan EA, Şahin S, Dilber B, Kurt T, Cansu A. 2018. The role of electroencephalography in differentiating epileptic and non-epileptic events in adolescents: A three-year experience of a

pediatric neurology center. Güncel Pediatri, 16(2):158-164.

Kazemi S, Katibeh P. 2018. Comparison of parametric and non-parametric EEG feature extraction methods in detection of pediatric migraine without aura. J Biomed Phys Eng, 8(3):305–314.

Kilic B. 2021. Evaluation of the Etiology, Clinical Presentation, Findings, and Prophylaxis of Children with Headache. Şişli Etfal Hospital Medical Bulletin, 55(1):128-133.

Klein A, Aeschlimann SA, Zubler F, Scutelnic A, Riederer F, Ertl M, et al. 2024. Alterations of the alpha rhythm in visual snow syndrome: A case-control study. J Headache Pain, 25(1):53.

Niedermeyer E, Lopes da Silva F. 2020. Electroencephalography: Basic principles, clinical applications, and related fields. 7th ed. Philadelphia: Lippincott Williams & Wilkins.

Ouyang CS, Hsiao FJ, Lo MT, et al. 2020. Quantitative electroencephalogram analysis of frontal cortex functional changes in patients with migraine. Kaohsiung J Med Sci, 36(7):543-551.

Petrušić I, et al. 2024. Machine learning classification meets migraine: Recommendations for study evaluation. J Headache Pain, 25:215.

Raghuraman L, Joshi SH. 2024. Application of EEG in the diagnosis and classification of migraine: A scoping review. Cureus, 16(7):e64961.

Reddy A, Reddy A. 2025. Migraine triggers, phases, and classification using machine learning models. Front Neurol, 16:1555215.

Rho YI, Kim JS, Kim DW, Choi SA, Lim BC, Chae JH, et al. 2020. EEG characteristics and diagnostic implications in childhood headache: A multi-center study. Front Neurol, 11:582516.

Rocca MA, Messina R, Colombo B, Falini A, Comi G, Filippi M. 2014. Structural brain MRI abnormalities in pediatric patients with migraine. J Neurol, 261(2):350-357.

Sadeghi S, Maleki A. 2018. Recent advances in hybrid brain-computer interface systems: A technological and quantitative review. Basic Clin Neurosci, 9(5):373.

Subasi A, Ahmed A, Aličković E, Hassan AR. 2019. Effect of photic stimulation for migraine detection using random forest and discrete wavelet transform. Biomed Signal Process Control, 49:231-239.

Vapnik V. 1995. The nature of statistical learning theory. New York: Springer Verlag.

Internet References

1- https://www.tutorialspoint.com/artificial_neural_network/artificial_neural_network_basic_concepts.htm (09.07.2025)